

This document was prepared in conjunction with work accomplished under Contract No. DE-AC09-76SR00001 with the U.S. Department of Energy.

### **DISCLAIMER**

This report was prepared as an account of work sponsored by an agency of the United States Government. Neither the United States Government nor any agency thereof, nor any of their employees, makes any warranty, express or implied, or assumes any legal liability or responsibility for the accuracy, completeness, or usefulness of any information, apparatus, product or process disclosed, or represents that its use would not infringe privately owned rights. Reference herein to any specific commercial product, process or service by trade name, trademark, manufacturer, or otherwise does not necessarily constitute or imply its endorsement, recommendation, or favoring by the United States Government or any agency thereof. The views and opinions of authors expressed herein do not necessarily state or reflect those of the United States Government or any agency thereof.

This report has been reproduced directly from the best available copy.

Available for sale to the public, in paper, from: U.S. Department of Commerce, National Technical Information Service, 5285 Port Royal Road, Springfield, VA 22161, phone: (800) 553-6847, fax: (703) 605-6900, email: [orders@ntis.fedworld.gov](mailto:orders@ntis.fedworld.gov) online ordering: <http://www.ntis.gov/ordering.htm>

Available electronically at <http://www.doe.gov/bridge>

Available for a processing fee to U.S. Department of Energy and its contractors, in paper, from: U.S. Department of Energy, Office of Scientific and Technical Information, P.O. Box 62, Oak Ridge, TN 37831-0062, phone: (865) 576-8401, fax: (865) 576-5728, email: [reports@adonis.osti.gov](mailto:reports@adonis.osti.gov)

TECHNICAL DIVISION  
SAVANNAH RIVER LABORATORY

DPST-86-695

DISTRIBUTION

- |                             |                                  |
|-----------------------------|----------------------------------|
| 1. J. D. Spencer, 773-A     | 9. R. L. Sindelar, 773-41A       |
| 2. M. H. Shearon, 703-A     | 10. G. A. Abramczyk, 773-41A     |
| 3. M. M. Anderson, 703-A    | 11. R. S. Ondrejcin, 773-A       |
| 4. W. E. Jule, 773-A        | 12. A. F. Riechman, 730-A        |
| 5. D. A. Mezzanotte, 779-2A | 13. N. P. Baumann, 773-41A       |
| 6. E. H. Perez, L-1307      | 14. E. W. Baumann, 773-A         |
| 7. G. R. Caskey, 773-41A    | 15. N. G. Awadalla, 773-41A      |
| 8. F. J. McCrosson, 773-41A | 16. SRL Records (2) PTERM, 773-A |

September 23, 1986

TO: W. E. JULE, 773-A

SRL  
RECORD COPYFROM: *N.G. Awadalla R.L. Sindelar G.A. Abramczyk/ky NGA*  
N. G. AWADALLA, R. L. SINDELAR, G. A. ABRAMCZYK, 773-41A

Q. A. REVIEW:

*G.R. Caskey, Jr.*  
G. R. Caskey, Jr.**REACTOR MATERIALS PROGRAM  
FRACTURE TOUGHNESS OF TYPE  
304 STAINLESS STEEL**INTRODUCTION

Task 5 of the Reactor Materials Program<sup>1</sup> (RMP) is designed to address the structural integrity of the SRP reactor tanks and moderator piping. The primary method to assess the structural integrity and to quantify the margins of safety is to perform detailed fracture assessment of the tanks and piping. A complete fracture assessment requires detailed knowledge of 1) component stresses including applied and residual stress distributions; 2) flaw sizes and distribution within the system and 3) material strength and toughness properties. The RMP provides a comprehensive program to address all the above issues. This report will focus on material toughness considerations, experimental procedures, specimen size effects and the use of the toughness results in the fracture assessment.

## SUMMARY

The experimental procedure for Type 304 Stainless Steel fracture toughness measurements and the application of results are described. Typical toughness values are given based on the completed test program for the RMP. Test specimen size effects and limitations of the applicability in the fracture mechanics methodology are outlined. A brief discussion on irradiation effects is given.

## DISCUSSION

### BACKGROUND

SRP reactor tanks and process piping are fabricated from tough, ductile material (Type 304 Stainless Steel). This material generally undergoes significant plastic deformation and crack tip blunting prior to initiation of crack growth. With these material characteristics, crack growth initiation is followed by stable growth. Hence, the maximum load that the structure can carry may be appreciably greater than the load that causes the initiation of growth. Under these conditions, a safety analysis of a degraded component should give explicit consideration to crack tip plasticity and fracture instability after some stable crack growth.

Conventional fracture mechanics techniques assume linear elastic behavior which ignores crack tip plasticity. Linear Elastic Fracture Mechanics (LEFM) can take into account a rising crack resistance during stable growth, but its predictions may give misleading estimates of the structure load carrying capability. Clearly, more appropriate fracture techniques are needed to avoid this situation. Several of these approaches have been investigated during the 1970's. Some of these approaches include:

- the J-resistance curve
- the crack tip opening angle criterion
- plastic collapse
- other approaches combining features of the above.

The focus of this paper is on the J-integral approach, used to develop the J-R curve.

### THE J INTEGRAL

Since its inception in 1968, the J-integral has been widely used as a fracture criterion in ductile fracture. Rice<sup>2</sup> proposed

a path-independent integral, the J-integral, which characterizes the elastic-plastic energy stored in the vicinity of a crack tip. Under the restriction of non-linear elasticity for a two dimensional deformation field (See Figure 1), the J-integral is defined as:

$$J = \int_{\Gamma} [W dx_2 - T \frac{\delta U}{\delta x_1} ds] \quad (1)$$

where:

- W is the strain energy density function
- $\Gamma$  is an integration path surrounding the crack tip (counterclockwise)
- T is the surface traction
- U is the displacement.
- ds is an element along the integral path
- $x_1$  and  $x_2$  are rectangular cartesian coordinates along and perpendicular to the crack axis.

Rice has also shown that for a sharp crack in a linearly elastic material and under the condition of plane strain, the J-integral reduces to the strain energy release rate,  $G_I$  or

$$J = \frac{(1-\mu^2) K_I^2}{E} = G_I \quad (2)$$

where

- $K_I$  is the "opening mode" stress intensity factor
- $\mu$  is Poisson's ratio
- E is the modulus of elasticity.

In the presence of small scale plastic yielding which does not perturb significantly the linear elastic state of stress, the J-integral can also be approximated by the strain energy release rate during crack extension.

For Type 304 SS, many researchers have developed techniques to characterize the J-integral and estimate its value experimentally. Several ASTM standards have also been developed to test specimens and to quantify the J-integral as a ductile fracture criterion.

#### EXPERIMENTAL EVALUATION OF J-INTEGRAL

ASTM standards E 399 and E 813 have been written to guide the testing of materials to determine fracture toughness. The

geometry of an ASTM standard Compact Tension (CT) Specimen is shown in Figure 2. The size of the specimen may be changed providing the scaling of all dimensions is maintained. In situations where one dimension may not be increased proportionally with the others, such scaling is justified where the critical dimension matches the actual material dimension, i.e. the specimen is the same thickness as the pipe or vessel wall.

Testing of CT specimens<sup>3</sup> is in terms of applied load versus displacement along the load line. Either single or multiple specimens may be used to determine the J-integral. A minimum of four individual specimens must be used, or four crack length measurements must be taken on the single specimen, within the specified range to determine  $J_{IC}$ . Specimens are fatigue precracked to a crack length not less than 0.76mm with a maximum permissible load not exceeding one fourth the specimen limit load,  $P_L$ , where  $P_L$  is defined as:

$$P_L = Bb^2\sigma_f / (2W+a) \quad (3)$$

where B, b, W and a are the specimen dimensions as shown in Figure 2

and

$\sigma_f$  is the flow stress and is defined as the average of the yield strength in tension (offset by 0.2%) and the tensile (ultimate) strength.

For multiple specimen tests, each specimen is loaded to a predetermined displacement value and immediately unloaded to zero load. The load-line displacement versus load is recorded. For single specimen tests, the data acquisition system must continuously record load versus load line displacement. The crack front is then marked so the crack growth during the test can be measured. Heat tinting is one method of marking. Heating the specimen in air to 200 to 300°C will clearly mark the entire crack surface. The specimen is then broken completely in two.

Once the specimen is apart, the original precrack length,  $a_0$ , and the crack growth,  $\Delta a$ , are measured. Each is measured at a minimum of nine positions across the fracture surface. These points accurately represent the crack growth when significant crack growth tunneling occurs. For a single specimen test, electrical potential measurements provide an average value of  $\Delta a$  representative of the whole crack front by measuring the response

of the specimen as a whole. The electrical potential method is comparable to the standard method, which is based on the average  $\Delta a$  measurements of the crack front.

J is calculated from the load versus load-line displacement records by:

$$J = (2A/Bb) [(1+\alpha)/(1+\alpha^2)] \quad (4)$$

where

$$\alpha = \sqrt{(2a_0/b)^2 + 2(2a_0/b) + 2 - (2a_0/b + 1)} \quad (5)$$

and

A is the area under the load versus load-line displacement curve

B is the specimen thickness (Figure 2)

b is the remaining ligament length of the specimen (Figure 2)

$a_0$  is the original or precrack length (Figure 2)

To establish a valid  $J_{IC}$  value, it is necessary to first develop a J versus  $\Delta a$  R curve, as shown in Figure 3. The  $J_Q$  point is then obtained from the intersection of a linear fit to the data (the R line) and a theoretical crack blunting line. For each data point calculate the value:

$$24(J/\sigma_f) \quad (6)$$

If this quantity is less than the original Bb value of the specimen, then the data point may be considered as a candidate for use in the R curve. At least four points are required to develop the R curve. On the axis of J versus  $\Delta a$ , draw a blunting line in accordance with the equation

$$J = 2\sigma_f \Delta a \quad (7)$$

At an offset of 0.15mm draw a minimum crack extension line parallel to the blunting line and at an offset of 1.5mm draw a maximum crack extension line parallel to the blunting line, as shown in Figure 4. With the method of least squares, determine a linear equation of the regression of J by using only those data points that fall within the minimum and maximum crack extension lines. This linear fit is the R line. The value of J at the intersection of the R line and the blunting line is  $J_Q$ .

The value  $J_Q$  is considered a valid  $J_{IC}$  value if the following criteria are met: (1) the minimum amount of crack extension must be to the right of the intersection of minimum crack extension

line and the R-line; (2) the minimum amount of crack extension must be less than one third of the horizontal distance from the blunting line to the data point of maximum  $\Delta a$ ; (3) the maximum amount of crack extension must lie to the left of the intersection point of the R line with the maximum crack extension line; (4) B must be greater than  $25J_Q/\sigma_f$ .

Figure 5 shows the various stages of crack growth and how the defined material property J relates to the material. The initial flaw without stress exists as a sharp crack. As the applied stress increases the tip of the crack blunts to a semicircular shape with some growth in length. At the onset of stable crack growth,  $J_{Ic}$  is defined as the J at the initiation of stable crack growth.

Crack growth stability is evaluated by comparing the applied tearing modulus against its material counterpart. For stable crack growth this is expressed as:

$$(dJ/da) * (E/\sigma_f^2) < (dJ_m/da) * (E/\sigma_f^2) \quad (8)$$

where the term on the left side of the inequality is the applied tearing modulus,  $T_{app}$ , and the right side term is the material counterpart,  $T_m$ . The term  $dJ/da$  is the slope of the J-R curve (at J greater than  $J_{Ic}$ ) illustrated in Figure 5.  $E/\sigma_f^2$  is a normalizing term which was originally introduced with  $dJ/da$  to alleviate the temperature dependence of the resistance curve. The flow stress,  $\sigma_f$ , is usually defined as one-half the sum of the yield and ultimate strengths and E is the elastic modulus. Equation (3) is usually written as:

$$T_{app} < T_m \quad (9)$$

for stability of crack growth.

#### RMP FRACTURE TOUGHNESS EXPERIMENTS

Table I lists the types and number of CT specimens used in the RMP. It should be noted that all specimens, except those in the HFIR IQ capsule, were made from Type 304 Stainless Steel plate taken from R Reactor piping. This provides us with 1950's vintage steel which is representative of the reactor pipes and tanks.

The larger planform was chosen for the corrosion testing specimens to allow a greater amount of crack growth than the .394T specimens. The smaller specimens are the largest size which would possibly fit into the various irradiation capsules.

### SPECIMEN SIZE EFFECTS

The design of the RMP CT specimens was based on a size effect variation study performed by Hanford Engineering Development Laboratory (HEDL) and geometry studies conducted by Materials Engineering Associates (MEA). The pipe material from which the RMP specimens were cut was 16 inch diameter by 1/2 inch wall thickness. Allowing for the curvature of the pipe and machining the faces of the specimens the maximum possible specimen thickness was .4 inches. A .394 inch (1 cm) specimen thickness was chosen. Decreasing the planform dimensions while holding the thickness constant gives greater toughness ( $J_{IC}$ ) values. This means the smaller planform specimens are less conservative.

Side grooving, which is used to provide a uniformly flat crack face after precracking, has the opposite effect. As the depth of the side-groove is increased, for the same size specimen, the  $J_{IC}$  value decreases. So side-grooving is a more conservative process. No study was done to correlate a small side-grooved specimen with a large unside-grooved specimen. All results are comparable within the same proportional configuration; same thickness, planform and depth of side-groove. A study with single-edge-notch cantilever specimens found no significant effect of thickness (.3 to 1.0 inches) on fatigue crack propagation rates in type 304 SS in temperatures from 75 to 1100 F. Also, crack growth rate data obtained from 1/2T CT specimens were essentially the same.

A typical  $J_{IC}$  curve is shown in Figure 6. A summary of  $J_{IC}$  values for the unirradiated material is shown in Figure 7. Note the wide range in  $J_{IC}$  values for the baseline material. The fracture surfaces of specimens have been examined for failure mode and photographed with a scanning electron microscope (SEM). All specimens exhibited ductile fracture.

### ELASTIC-PLASTIC FLAW STABILITY ANALYSIS PROCEDURES

The analysis used to determine part-throughwall and throughwall instability conditions are based on the  $J$ -integral and the associated tearing modulus,  $T$ , instability criterion. There are three basic considerations in the tearing modulus ( $J/T$ ) approach. The first consideration, requires the equilibrium between the potential to extend an existing crack, typically written as  $J$  in the literature, and the material resistance to crack extension,  $J_m$ . The equilibrium condition is expressed mathematically as:

$$J = J_m(\Delta a). \quad (10)$$

J is a measure of the elastic-plastic stress-strain field around the crack tip field for any specified crack geometry and loading. J expressions have been developed for various flaw geometries and loadings. J depends on the geometry of the flawed component, flaw shape, orientation, and size, and loading type (tension, bend, etc.). J also depends upon the material stress-strain relationship as it dictates the extent of plasticity in the vicinity of the crack tip.

The material resistance to crack extension, typically referred to as the J-R curve and illustrated in Figure 5, is considered to be material property for a specific heat of material, temperature, and a crack-related condition called plane strain. In reality, however, J-R curves are also often found to depend upon parameters such as type of loading (tension or bend), crack geometry, and component thickness. In the J-R curve shown in Figure 5,  $J_C$  refers to the onset of extension of the existing crack. When the plane strain conditions are satisfied, initiation J is denoted by  $J_{IC}$ . The plane strain crack condition generally provides a lower bound behavior for material resistance to stable crack growth.

The second consideration in the tearing modulus approach is that proportional loading of the crack tip field must be satisfied during crack growth. The condition for the proportional loading (J controlled growth) is:

$$(dJ/da) * (b/J) \gg 1, \quad (11)$$

where b is the remaining ligament, and the term on the left side of the inequality generally is denoted as  $\omega$ . When  $\omega$  is greater than 10 J-controlled growth requirements are satisfied and the J/T theory is applicable. This requirement must at least be satisfied by the J-resistance curve. Generally, only small amounts on crack growth are allowed under the strict requirements of J-controlled growth.

The third aspect of the J/T approach concerns stability of a growing crack. While Equation (10) provides a means for inferring crack growth from the J-resistance curve, it does not define stable crack growth. The above discussion on crack stability is an extension of the graphical approach used in linear elastic fracture mechanics (LEFM) methods. In LEFM methods, crack instability is normally evaluated under load controlled conditions. The tearing modulus concept extended this idea to more realistic conditions such as a displacement controlled loading for a compliant system. The displacement controlled loading is one where displacements (rotations) at certain reference locations are

held fixed while examining crack growth stability. Such loading allows system characteristics to be readily incorporated into the tearing instability analysis.

### J-T DIAGRAM

A convenient means to define the margin against instability involves plotting  $J$  ( $>J_{IC}$ ) as a function of  $T$  for the applied and material resistance values. This J-T diagram is shown schematically in Figure 8. Here, the material curve is developed from a J-R curve illustrated in Figure 5. If the applied load, crack length, and system parameters are such that the applied  $T$  curve intersects the material curve, then crack instability is predicted. The amount of stable crack growth before instability is then inferred using the  $J$  value at point I and the J-resistance curve in Figure 5.

The J-T Diagram is used within two bounding limits. If the applied  $J$  is below  $J_{IC}$ , the crack stability is automatically assured because crack growth is not implied. The upper bound limit for J-controlled growth illustrated as point L on the J-T diagram (Figure 8a). Beyond point L, the inequality in equation (11) may not be satisfied and the tearing stability methods can be applied only approximately and the analyst must use caution in interpreting results.

### LOW TEMPERATURE IRRADIATION EFFECTS ON FRACTURE TOUGHNESS:

Neutron irradiation alters the mechanical properties of metals, the response being strongly temperature and fluence dependent. Irradiation of Type 304 Stainless Steel at temperatures near  $100^{\circ}\text{C}$  is known to cause radiation hardening, characterized by an increase in strength and decrease in ductility<sup>8-11</sup> and a decrease in impact energy<sup>12</sup>. No data on the fracture toughness of Type 304 Stainless Steel irradiated at  $100^{\circ}\text{C}$  have been reported. However, estimates of the fracture toughness as a function of fast fluence have been made<sup>13</sup> using a correlation between Charpy V-Notch (CVN) values and J-integral crack resistance data developed for ferritic steels<sup>14,15</sup>. It is predicted that the toughness (characterized by  $J_{IC}$ ) will decrease monotonically up to  $10^{20}$  -  $10^{21}$  n/cm<sup>2</sup> ( $E > 0.1$  MeV)<sup>16</sup> and remain relatively constant to  $10^{22}$  n/cm<sup>2</sup>.

Irradiation of .4T CT specimens in the High Flux Isotope Reactor will provide toughness data at fluences ranging from  $3 \times 10^{20}$  -  $1 \times 10^{22}$  n/cm<sup>2</sup> ( $E > 0.1$  MeV). These values span the current and future ( $>50$  years) fast fluence levels in the SRP reactor walls under the current mode of operation.

It is difficult to predict the effect of irradiation on the strength properties of these materials. Tensile tests indicate that the yield and ultimate strength values may reach a saturation value where increasing fluence has little further detrimental effect on the material. If the same were true for compact tension tests, it would be possible to assume the residual strength of the P, K, and L Reactor tanks from the material data obtained from the R Reactor CT specimens. However, the existence of a  $J_{Ic}$  saturation level has not been proven to date.

GAA/NGA/RLS:elr

REFERENCE

1. N. G. Awadalla, G. R. Caskey, Jr., and R. S. Ondrejcin, "Reactor Materials Program," DPST-84-820 (December, 1984).
2. J. R. Rice, "A Path Independent Integral and the Approximate Analysis of Strain Concentration by Notches and Cracks," Journal of Applied Mechanics (June, 1968).
3. G. A. Clarke, et al., "A Procedure for the Determination of Ductile Fracture Toughness Values Using J Integral Techniques," Journal of Testing and Evaluation, JTVEA, Vol. 7, No. 1, Jan. 1979, pp. 49-56.
4. W. J. Mills, "Effect of Specimen Size on the Fracture Toughness of Type 304 Stainless Steel -- Interim Report," HEDL-TME 81-52 (February, 1982).
5. J. R. Hawthorne, et al., "Sample Preparation, Irradiation, and Testing of 304 Stainless Steel Specimens," Materials Engineering Associates monthly report MEA-85-13.
6. J. R. Hawthorne, et al., "Sample Preparation, Irradiation, and Testing of 304 Stainless Steel Specimens," Materials Engineering Associates monthly report MEA-85-20.
7. P. Shahinian, Naval Research Laboratory, "Influence of Section Thickness on Fatigue Crack Growth in Type 304 Stainless Steel," Nuclear Technology Vol. 30 (September 1976).
8. J. W. Joseph, "Mechanical Properties of Irradiated Welds in Stainless Steel," DP534 (December, 1960).
9. J. W. Joseph, "Stress Relaxation in Stainless Steel During Irradiation," DP-368 (June, 1959).
10. E. E. Bloom, et al, "The Effect of Irradiation Temperature on Strength and Microstructure of Stainless Steel," Jnl Nuc Mat. 22 68, (1967).
11. H. R. Higgy and F. H. Hammad, "Effect of Fast-Neutron Irradiation on Mechanical Properties of Stainless Steel," Jnl Nuc Mat. 55 177 (1975).
12. J. R. Hawthorne, et al., "Sample Preparation, Irradiation, and Testing of 304 Stainless Steel Specimens," Materials Engineering Associates monthly report MEA-85-15.

13. G. R. Caskey to W. E. Jule, "Fracture Toughness Estimates - Irradiated Stainless Steel," (August, 1986).
14. J. R. Hawthorne, A. L. Hiser and F. J. Loss, "Projection of Postirradiation Fracture Toughness for 125°C Neutron Irradiated Type 304 Stainless Steel, "MEA 86-18 (MEA 2177), (August 12, 1986).
15. J. R. Hawthorne, F. J. Loss, R. G. Berggren and J. P. Gudas, "Resolution of the Task A-11, Reactor-Vessel Materials Toughness Safety Issue," NUREG-0744, Vol. 2, Rev. 1, Appendix D, Materials Toughness Properties.

TABLE 1

RMP CT SPECIMENS

Test Series	Mechanical Testing		Corrosion Testing	
	<u>.394T</u>	<u>.394x1T*</u>	<u>.394T</u>	<u>.394x1T</u>
Unirradiated	78	8		
HFIR Irradiation 4M, 4C, and 12M Capsules)	36		4	
HFIR Irradiation (1Q, F50 304 SS Plate)	18			
K Rx Surveillance	60			
Corrosion Studies				18
<u>TOTAL</u>	192	8	4	18

\* 1T-CT Planform, .394-in thick.

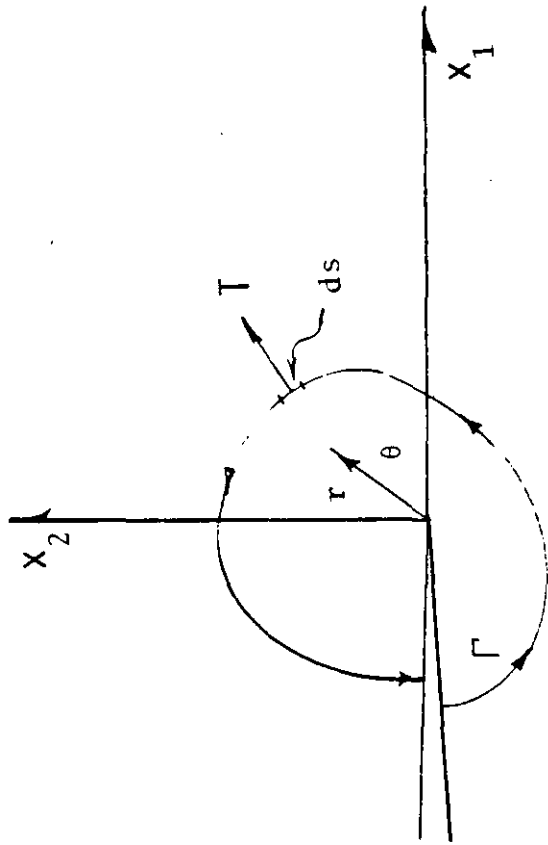


Figure 1 Expressions Used To Define J Integral

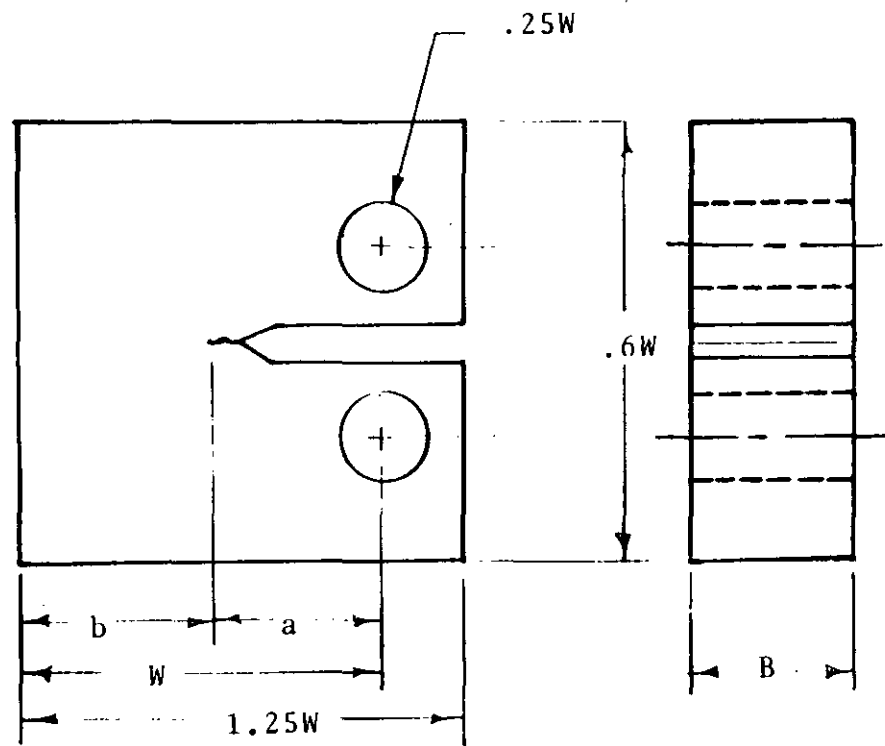


Figure 2 Compact Tension (CT) Specimen Standard Proportions

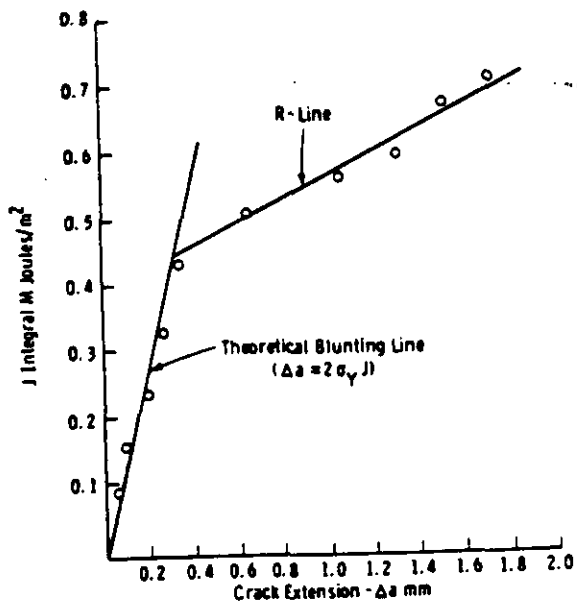


Figure 3 -Schematic of J versus Δa R curve showing best-fit R line and theoretical blunting line.

(Note: 1M J/m<sup>2</sup> = 5.7k inlb/in<sup>2</sup>)

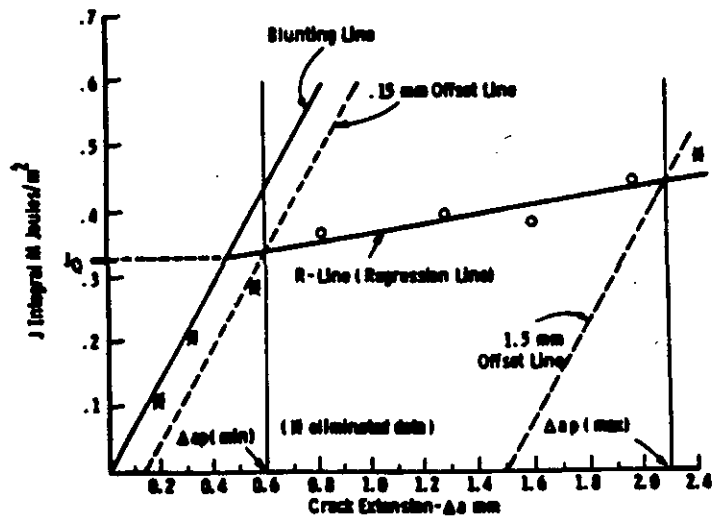


Figure 4 -Schematic of method used to determine  $J_0$  point.

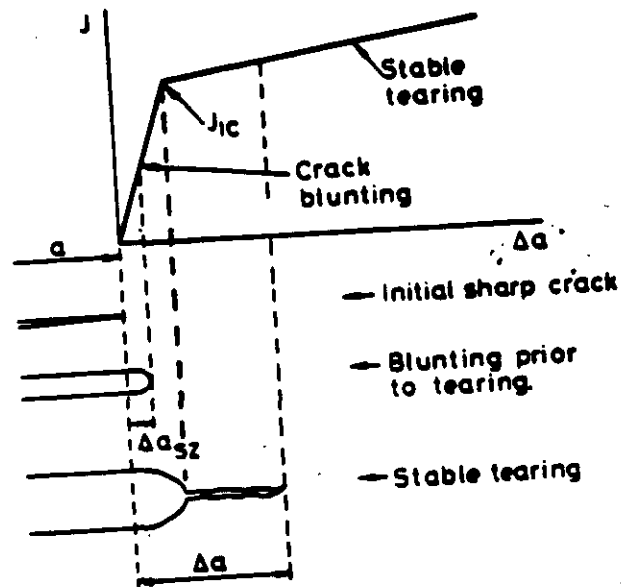
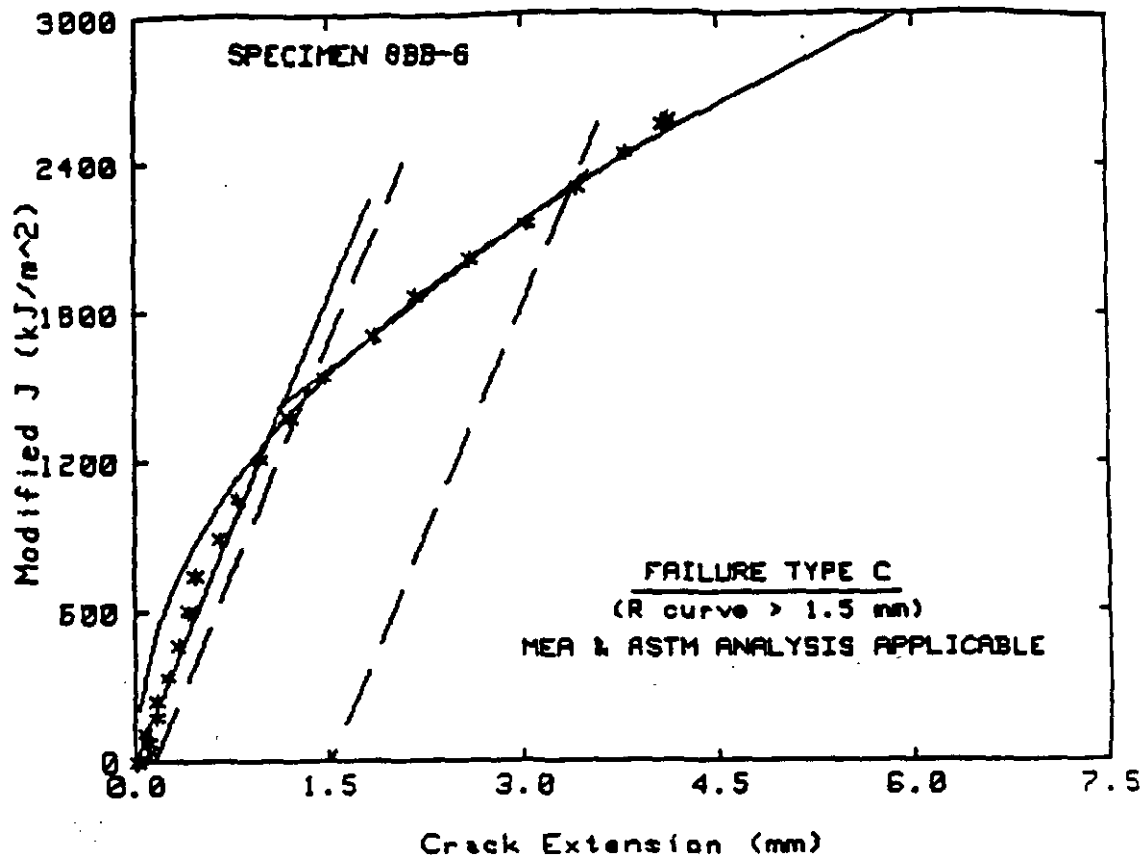


Figure 5 Definition of  $J_{1c}$ .



**TEST SPECIMEN DATA**

Material Type	= DUPONT RING 8	
Test Temperature	= 25 C	
Percent Side Groove	= 0 %	
Specimen Thickness	= 9.9822 mm	
Init crack length	= 11.31 mm	Init a/W = .565
Final crack length	= 16.23 mm	Final a/W = .811
Flow stress	= 620.5 MPa	(Estimated Value)
Youngs modulus	= 205700 MPa	(Estimated Value)

**POWER LAW DATA  $J = C (\Delta a)^N$**

J ( $\theta J/T=8.8$ )	= 1890.3 kJ/m <sup>2</sup>
J <sub>ic</sub>	= 1454.2 kJ/m <sup>2</sup>
K <sub>jc</sub>	= 547 MPa √m
Exponent N	= .4859
Coefficient C	= 1268.3 kJ/m <sup>2</sup>
T (average)	= 216

**LEAST SQUARE LINEAR LINE (ASTM)  $J = M (\Delta a) + B$**

J <sub>ic</sub>	= 1426.6 kJ/m <sup>2</sup>
K <sub>jc</sub>	= 541.8 MPa √m
Slope M	= 397868.4 kJ/m <sup>3</sup>
Intercept B	= 968.9 kJ/m <sup>2</sup>
T (ASTM)	= 213
Validity (J <sub>ic</sub> )	= INVALID--c (.82 vs .73), d, e
Validity (R-curve)	= INVALID--2, 3 (.82 vs .13)
J maximum allowed	= 269.2 kJ/m <sup>2</sup> (J <sub>max</sub> =B <sub>net</sub> *Flow stress/20)
Delta a max. allowed	= .87 mm (Delta a max = 0.1*bo)
Final Delta a	= 4.09 mm
Poisson's Ratio (ν)	= 0

Figure 6 Typical J-R Curve

TYPICAL UNIRRADIATED J<sub>1c</sub> DATA

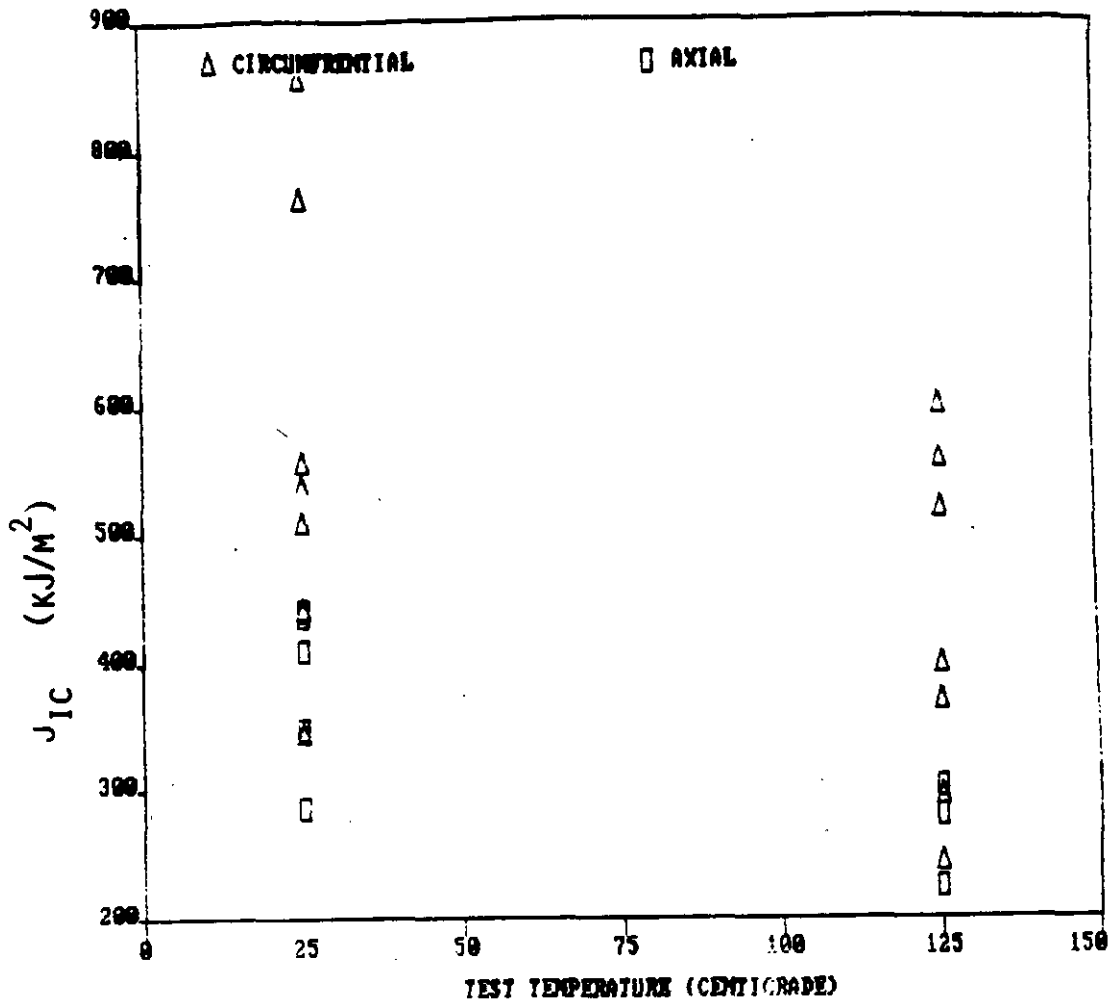


Figure 7 RMP Typical Unirradiated J<sub>1c</sub> Data

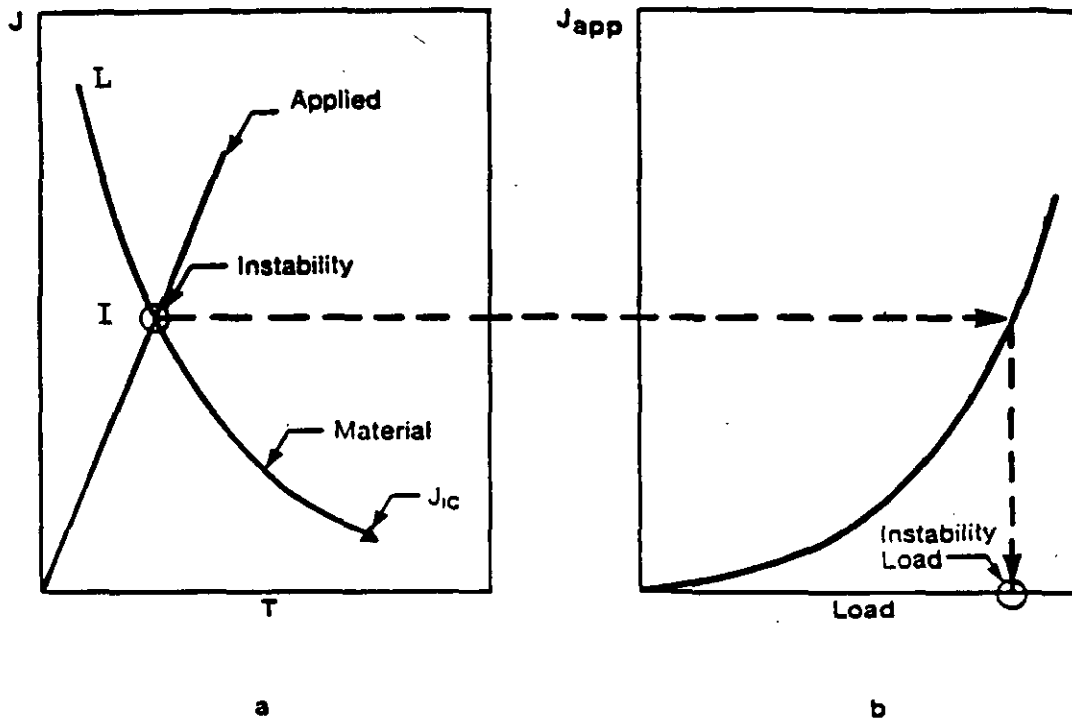


Figure 8  
 Illustration of Determination of the  
 Instability Load,  $J$ , and  $T$  Conditions